HHS Public Access

Author manuscript

J Mol Microbiol Biotechnol. Author manuscript; available in PMC 2018 September 27.

Published in final edited form as:

J Mol Microbiol Biotechnol. 2012 ; 22(5): 287–299. doi:10.1159/000342520.

The smallest active carbamoyl phosphate synthetase was identified in the human gut archaeon *Methanobtrevibacter smithii*

Elena Popa[1], **Nirosha Perera**[2], **Csaba Z. Kibédi-Szabó**[1], **Hedeel Guy-Evans**[2], **David R. Evans**[3], and **Cristina Purcarea**[1]

[1]Department of Microbiology, Institute of Biology Bucharest, Romanian Academy, Bucharest 060031, Romania

[2]Department of Chemistry, Eastern Michigan University, Ypsilanti, MI 48197, USA

[3]Department of Biochemistry and Molecular Biology, Wayne State University School of Medicine, Detroit, MI 48201, USA

Abstract

The genome of the major intestinal archaeon, *Methanobrevibacter smithii*, contains a complex gene system coding for carbamoyl phosphate synthetase (CPSase) composed of both full-length and reduced-size synthetase subunits. These ammonia-metabolizing enzymes could play a key role in controlling ammonia assimilation in *M. smithii*, affecting the metabolism of gut bacterial microbiota, with an impact on host obesity. In this study, we isolated and characterized the small (41 kDa) CPSase homolog from *M. smithii*. The gene was cloned, overexpressed in *E. coli*, and the recombinant enzyme was purified in one step. Chemical cross-linking and size exclusion chromatography indicated a homodimeric/tetrameric structure, in accordance with a dimer-based CPSase activity and reaction mechanism. This small enzyme, MS-s, synthesized carbamoyl phosphate from ATP, bicarbonate, and ammonia, and catalyzed the same ATP-dependent partial reactions observed for full-lenght CPSases. Steady state kinetics revealed a high apparent affinity for ATP and ammonia. Sequence comparisons, molecular modeling and kinetic studies suggest that this enzyme corresponds to one of the two synthetase domains of the full-length CPSase that catalyze the ATP-dependent phosphorylations involved in the three step synthesis of carbamoyl phosphate. This protein represents the smallest naturally occurring active CPSase characterized thus far. The small *M. smithii* CPSase appears to be specialized for carbamoyl phosphate metabolism in methanogens.

Keywords

carbamoyl phosphate synthetase; ancestral form; *Methanobrevibacter smithii*; intestinal archaea; evolution; obesity

Corresponding author: Dr. Cristina Purcarea, Department of Microbiology, Institute of Biology Bucharest, Romanian Academy, 296 Splaiul Independentei, 060031 Bucharest, Romania, cristina.purcarea@ibiol.ro, cri48223@yahoo.com, tel. (+40)746151081, FAX: (+40)212219071.

Introduction

In recent years, many studies [Dridi *et al.*, 2011, Horz and Conrads, 2010, Nava *et al.*, 2011, Plottel *et al.*, 2011] have focused on the involvement of the human microbiome in human health and disease. While archaea colonizes several different anaerobic niches within the human body [Belay *et al.*, 1988, 1990], there is a single predominant species, *Methanobrevibacter smithii*, present in the human gut [Miller *et al.*, 1982]. First isolated from feces, this methanogenic organism is a strict anaerobe that grows on a mixture of hydrogen and carbon dioxide [Balch *et al.*, 1979].

Samuel and Gordon made the remarkable discovery that a synergic interaction in the colon between *Methanobrevibacter smithii* and *Bacteroides thetaiotaomicron*, the major gut prokaryote, appears to have an important role in controlling host obesity [Samuel and Gordon, 2006]. Complex dietary polysaccharides that cannot be metabolized by the human host are digested by enzymes in the gut microbiome [Stams, 1994]. Bacterial fermentation of polysaccharides yields short chain fatty acids that provide as much as 10% of the daily caloric intake of the host. Archaeal methanogenesis facilitates bacterial fermentation by preventing the accumulation of H_2 gas and other end products that would otherwise inhibit the process. Analysis of the cecal content of gnotobiotic mice colonized with *M. smithii* alone or together with *B. thetaiotaomicron* revealed that many genes that participate in the metabolism of these end-products are up-regulated when both organisms are present in the gut [Samuel *et al.*, 2007]. Several lines of evidence suggest that obesity is associated with elevated levels of intestinal methanogenic archaea [Million *et al.*, 2011]. Consequently, *M. smithii* is considered to be a potential therapeutic target in the treatment of obesity [Buck and Hansen, 2007]. The principle source of nitrogen in *M. smithii* is ammonia, resulting from the degradation of amino acids by the host or intestinal bacteria. *M. smithii* competes with *B. thetaiotamicron* for the available ammonia, and when both organisms populate the gut, the transcription of several enzymes involved in ammonia transport and assimilation is up-regulated in *M. smithii*. Although there have been numerous microbiological and physiological studies of human gut microbiota, little is known about the metabolism and key enzymes of the major archaeon in the gastrointestinal tract, *M. smithii*.

Carbamoyl phosphate synthetase (CPSase; EC 6.3.5.5) plays a major role in ammonia assimilation in all organisms. The enzyme catalyzes the synthesis of carbamoyl phosphate (CP), a common precursor of pyrimidine nucleotides, arginine and, in terrestrial vertebrates, urea, where it represents the major means of eliminating ammonia. CPSases are multi-subunit or multidomain proteins. *E. coli* CPSase is composed of a 40 kDa glutaminase (CarA, GLN) subunit which hydrolyzes glutamine and transfers ammonia to a 120 kDa synthetase (CarB, SYN) subunit [Trotta *et al.*, 1971]. The SYN subunit consists of two homologous domains having a nearly identical tertiary fold and active site residues that were thought to have evolved by an ancestral duplication and fusion [Nyunoya and Lusty, 1983]. The amino half of the subunit, designated CPS.A, catalyzes the synthesis of carbamate from ATP, bicarbonate and ammonia, while the carboxyl half, CPS.B, catalyzes carbamoyl phosphate synthesis from carbamate and a second ATP [Post *et al*, 1990; Alonso and Rubio, 1995, Guy and Evans 1996]. *E. coli* CPSase GLN and SYN subunits associate to form heterodimers and tetramers [Anderson,1986]. The partial reactions catalyzed by CPSase,

first demonstrated for the *E. coli* enzyme [Anderson and Meister, 1965; Meister, 1989], are thought to occur universally in nearly all organisms:

CPS.A (1) ATP + bicarbonate → carboxy phosphate + ADP

(2) carboxy phosphate + NH_3 → carbamate + Pi

CPS.B (3) ATP + carbamate → carbamoyl phosphate + ADP

Each of the major CPSase domains are comprised of three subdomains designated A1, A2, A3 and B1, B2, B3 [Guillou *et al.*, 1989; Post *et al.*, 1990; Rubio *et al.*, 1991; Guy and Evans, 1996]. A The X-ray structure of *E. coli* CPSase [Thoden *et al.*, 1997] showed that the A1–A2 and B1–B2 subdomains have nearly identical tertiary folds. A2 and B2 are catalytic subdomains, catalyzing reactions 1–2 and 3, respectively [Post *et al.*, 1990; Guy *et al*, 1997; Thoden *et al.*, 1997]. The A3 and B3 subdomains have distinctly different tertiary structures and functions. B3 is a regulatory subdomain that has been adapted to bind allosteric ligands [Rubio *et al.*, 1991]. Remarkably, the active sites on the GLN, CPS.A and CPS.B domain are connected by a 96 Å long intramolecular tunnel that sequesters the labile intermediates within the *E. coli* enzyme complex [Thoden *et al.*, 1997].

Although the structural organization of the CPSases is very diverse, all are composed of homologous domains and subdomains and catalyze the same series of reactions. Generally, bacteria possess a single CPSase that catalyzes the formation of carbamoyl phosphate used for both arginine and pyrimidine nucleotides biosyntheses, while enteric and gram-positive bacteria contain two CPSases, each specific for one of these two metabolic pathways [Paulus and Switzer, 1979]. These enzymes are comprised of homologous SYN subunits of comparable size [Yang et al., 1997]. Most CPSases have a full length SYN subunit consisting of fused CPS.A-CPS.B domains, but there are several organisms, including the thermophilic archaeon *Methanocaldococcus jannaschii* [Bult *et al.*,1996] and the hyperthermophilic eubacterium *Aquifex aeolicus* [Ahuja *et al.*, 2001], that have a split *carB* gene encoding separate polypeptides corresponding to CPS.A and CPS.B domains. The only known exception is a 34 kDa carbamate kinase-like CPSase of entirely different sequence and tertiary structure found in the hyperthermophilic archaeon *Pyrococcus furiosus* [Legrain *et al.*, 1995, Durbecq *et al.*, 1997; Marina *et al.*, 1998, Uriarte *et al.*, 2001], and in *Pyrococcus abyssi* [Purcarea *et al.*, 1996, 2001].

The genome of *M. smithii* contains *carA* and *carB* genes coding for a 40 kDa GLN subunit and a 118 kDa SYN subunit (**MS-l, SYN1**), respectively, that are similar to the CPSase subunits found in most bacteria [Popa *et al.*, 2009]. Surprisingly, the genome also contains two genes coding for much smaller proteins that are homologous to the CPSase synthetase domain. One of these proteins (**SYN2**) consists of 391 residues (45 kDa) with a sequence that resembles a truncated CPS.B domain, but it lacks active site residues that are known to participate in substrate binding and catalysis. Therefore, it is likely to be encoded by an inactive pseudogene. The second small CPSase homolog (**MS-s, SYN3**) is also homologous to a part of CPS.B and consists of 367 residues (41 kDa) including the residues implicated in catalysis [Popa *et al.*, 2009]. Prior to this report it was not known whether this protein has catalytic activity or is an inactive remnant of an unproductive gene duplication event.

We have isolated and characterized the small *M. smithii* CPSase, MS-s, showing that it is catalytically active, synthesizing carbamoyl phosphate from NH_3, 2 ATP and bicarbonate by the same mechanism utilized by the large CPSases. This is the smallest functional CPSase discovered thus far and may more closely resemble the putative ancestral kinase that gave rise to this diverse family of enzymes.

Results and Discussion

Sequence analysis

The large SYN subunit of the CPSase from the methanogens, *M. smithii* (MS-l), *Methanothermobacter thermoautotrophicus* (MT-l) and *Methanosphaera stadtmanae* (MST-l) are 70–73% identical to one another (Figure 1B). The alignment of the *E. coli* CPSase SYN subunit with the large CPSases MS-l, MT-l and MST-l gave sequence identities of 50–53%, indicating that the CPSase from *E. coli* and methanogens are closely related to each other and to the SYN subunit of most prokaryotic and eukaryotic organisms.

The small CPSase from *M. smithii*, MS-s, is homologous to the CPS.B subdomain of *E. coli* but is significantly smaller, 367 vs 513 residues, respectively (Figure 1A), representing about of third of the full length subunit (1073 residues). Based on the deduced amino acid sequence, the protein has a calculated molecular mass of 41,403 Da, and an isoelectric point of 4.62. MS-s aligns with residues 560–947 of the *E. coli* SYN subunit corresponding to B1 and B2 subdomains of CPS.B [Goillou *et al.*, 1989] (Figure 1A) with a score of 20.1% sequence identity (Figure 1B), and therefore lacks the B3 subdomain at the carboxyl end of the polypeptide.

MS-s is also homologous to the *E. coli* CPS.A domain, as expected, since the CPS.A and CPS.B domains of the *E. coli* enzyme are quite similar to one another (19.3% identity, 34.5% similarity). However, the alignment score of MS-s is somewhat higher for CPS.B (20.1% identity, 40.1% similarity) than for CPS.A, and the modeling program selected CPS.B as the best structural template. By analogy to the function of B3 in other CPSases, which have binding sites for both allosteric activators and inhibitors [Goillou *et al.*, 1989, Rubio *et al.*, 1991; Guy and Evans, 1996; Fresquet *et al.*, 2000], the lack of this domain in MS-s suggests that this enzyme is unregulated.

Open reading frames encoding large and small putative CPSases found in *M. smithii* are also present in the genomes of the thermophilic archaeon *Methanothermobacter thermoautotrophicus* and in the human intestinal archaeon *Methanosphaera stadtmanae*, therefore this unusual complement of CPSase genes may represent a common feature of methanogens. The overall sequences of the small CPSases from these three methanogens are well conserved (46.9–48.1% identity), and are much less similar to the synthetase domain of *E. coli* CPSase (20.1–25.3% identity).

Moreover, the deduced aminoacid sequence of the small *M. smithii* CPSase has a limited overall identity score (19.1–24.2%) with the corresponding SYN subunits of full-length CPSases from *E. coli* and methanogens, but an appreciably higher identity score (47.6–48.1%) with the small CPSases from methanogens (Figure 1B). The large SYN subunit of

the CPSase from the methanogens *M. smithii* (MS-l), *M. thermoautotrophicus* (MT-l) and *M. stadtmanae* (MST-l) are 70–73% identical to one another (Figure 1B). The alignment of the *E. coli* CPSase SYN subunit with the large CPSases MS-l, MT-l and MST-l gave sequence identities of 50–53%, indicating that the full length CPSases from *E. coli* and methanogens are closely related to each other and to the SYN subunit of most prokaryotic and eukaryotic organisms.

Since both MS-s and the CK-like CPSases are small CP-synthesizing enzymes having molecular mass of 41 kDa and 33 kDa, respectively, we investigated the possibility that MS-s may be more closely related to the CK-like CPSases than to the larger forms of the SYN CPSase subunits found in most bacteria. However, while the percent identity between MS-s and *E. coli* CPSase is relatively low, 20.1%, the percent identity between the MS-s and *P. abyssi* CK-CPSase is only 11.5%. This difference is highly significant at these low levels of sequence similarity. Four randomized versions of the *P. abyssi* CK-CPSase sequence were generated of identical in size and amino acid composition but a completely unrelated amino acid sequences. Sequence alignments yielded a percent identity between MS-s and the four randomized *P. abyssi* proteins of 7.4%, 13.0%, 14.1% and 15.1%. This analysis suggests that MS-s and *P. abyssi* CPSase matches are coincidental and that the proteins are not homologs. This interpretation was reinforced by the conservation of *E. coli* CPSase active site residues and the kinetic studies described below.

The calculated phylogenetic tree (Figure 2) illustrates the relationship between the CPSase SYN subunit from methanogens, *E. coli* and other organisms belonging to all three domains of organisms, Bacteria, Archaea and Eukarya. The small CPSases from the methanogens were the first to diverge, forming a separate branch. These proteins are more distantly related to the other bacterial, archaeal and eukaryotic CPSases. Distinct branches cluster the eukaryotic CPSases from yeast (SC) and mammals (CAD), the archaeal large CPSases, and the bacterial full-length CPSases. One unanticipated result is that CPSase from *A. aeolicus* (AA), an organism of ancient lineage which has a split gene encoding separate CPS-A and CPS-B polypeptides [Ahuja *et al.* 2001], is a close relative of *E. coli* CPSase and other bacterial CPSases. Interestingly, the large methanogenic CPSases cluster together forming a separate lineage distinct from other bacterial and archaeal enzymes. The carbamate kinase-like CPSase from *P. abyssi* (PA) [Purcarea *et al.*, 2001] is located on a distant branch of the phylogenetic tree, consistent with its distinctive sequence and structure.

The residues involved in substrate binding and catalysis in MS-s were identified based on X-ray structural analysis of *E. coli* CPSase with a non-hydrolyzable ATP analog [Thoden *et al.*, 1999]. The alignment of *M. smithii* MS-s with the *E. coli* CPS.B and CPS.A domains (Figure 3) showed that all of the putative active site residues from one or the other domain have been conserved. The only exception is Arg848 in *E. coli* CPS.B that has been replaced in the archaeal enzyme by Gly274.

All of the active site residues identified in the X-ray structure of *E. coli* CPSase with a nonhydrolyzable ATP analog bound [Thoden *et al.*, 1999], are located between residues 129 to 306 of the A2 subdomain and 677–848 of the B2 subdomain (Figure 3). Sequence alignment showed that of the twelve active site residues in CPS.A, which catalyze carbamate

formation (reactions 1 and 2), all are conserved in the corresponding positions in CPS.B, which catalyzes carbamoyl phosphate synthesis (reaction 3). This high degree of conservation is consistent with the similarity of the reactions catalyzed by the two domains: ATP dependent phosphorylations of bicarbonate and carbamate. The substrates are isosteric, the only difference is that one of the oxygens in bicarbonate is replaced by an N-H in carbamate. When MS-s is included in the sequence alignment, ten of these same twelve residues were found to be identical or highly conservative substitutions (K/R or L/I) with residues in CPS.A and/or CPS.B. Two MS-s residues, Asp253 and Gly274, are not conserved (Figure 3), but these are interactions with the backbone amide, not the side chain. As will be subsequently discussed, the alignments are consistent with the observation that MS-s can catalyze both carbamate and carbamoyl phosphate formation (reactions 1–3). It is significant that the putative active site residues are nearly perfectly conserved while the overall sequence identity to the *E. coli* subdomains is only 20%.

Molecular Modeling

Modeling of the three dimensional structure of MS-s was attempted using Modeller9v9. The three dimensional model was computed using the X-ray structure of *E. coli* CPSase SYN subunit (pdb: 1BXR) as a template. The program fit (Figure 4) MS-s to the B1–B2 subdomains of the carbamate phosphorylation domain (CPS.B). The Ramachandran plot of the model structure indicated that 95.6% of the residues are in most favored or allowed regions, 2.2% in generously allowed regions, and 2.2% in disallowed regions (data not shown). Due to the low sequence identity between MS-s and *E. coli* B1–B2 (20%), the model statistics were poor (the ERRAT2 score of 74 and the Z score (ProSa) of −5.78), precluding an accurate positioning of MS-s active site residues. However, the superposition of the model with *E. coli* CPSase gives an rmsd of 1.66 Å for 144 α-carbons and 1.66 Å for backbone atoms, suggesting that the overall tertiary fold is likely to be approximately correct.

Cloning, expression and purification of recombinant MS-s

M. smithii ATCC 35061 (DSM 861) cells were grown anaerobically at 37°C using H_2:CO_2 gas mixture, as described in the *Experimental Procedures*. Under these conditions, the culture reached the stationary phase after 200 hours (data not shown). Chromosomal DNA was isolated in the presence of mutanolysin, as described in the *Experimental Procedures*, yielding 86.5 mg/ml archaeal DNA. The MS-s *carB* gene (YP_001273061) coding for the *M. smithii* 367-residue CPSase was amplified by PCR, and the resulting DNA fragment was inserted into the pRSETC expression vector, using *Bam*HI-*Nco*I restriction sites. This vector allows the expression of the recombinant CPSase with a 3 kDa Histag fused to the amino end of the protein. The resulting plasmid (pMS-s) was analyzed by double digestion with the cloning restriction enzymes *Bam*HI-*Nco*I, and both strands were sequenced.. The construct, pMS-s encoding MS-s was expressed in *E. coli* BL21(DE3) by IPTG induction at 20°C, and the recombinant MS-s was purified from the soluble fraction in a single step, by Ni^{2+}-affinity chromatography (Figure 5A), as indicated in the *Experimental Procedures*. The yield of the purified recombinant MS-s obtained was 14 mg/l of culture. SDS-PAGE analysis of the purified protein gave the expected molecular mass of 44 kDa, taking into consideration the fused 3-kDa His-tag polypeptide.

Oligomeric structure

The oligomeric structure of MS-s was assessed by chemical crosslinking with dimethyl suberimidate [Davies *et al.*, 1970]. The time course of the crosslinking reaction (Figure 5B) shows that monomeric MS-s gradually disappeared as the reaction proceeded, and was converted into two discrete high molecular species, possibly a tetramer and a higher oligomeric species. The formation of sharp bands in the gels argues against non-specific association of the monomers which would tend to give a broad, highly heterogeneous species forming a smear.

E. coli CPSase monomers associate to form dimers and tetramers [Kim and Raushel, 2001]. Since, MS-s is homologous to the truncated CPS.B domain, the dimer would correspond to full length CPS.A-CPS.B synthetase *monomer* without the A3 and B3 subdomains. The MS-s tetramer would be equivalent to a dimer of the *E. coli* synthetase domain again without A3 and B3. The expected molecular mass of the MS-s dimer and tetramer would be 88 and 176 kDa, respectively, taking into account the appended 3-kDa His-tag polypeptide. The failure to observe the dimeric species is not unusual during chemical crosslinking, and can occur if the residues involved in forming the crosslinks are not optimally positioned so that the rate of crosslinking of the tetramer and higher oligomers occurs much more rapidly than the dimer.

The oligomeric structure of MS-s was further investigated by size exclusion chromatography on a calibrated Hiload 16/60 superdex 200 column (Figure 5C). Two protein peaks were observed by measuring the absorbance at 280 nm and SDS-PAGE analysis. Calibration of the column with known proteins gave a molecular mass of 91 kDa and 185 kDa for these two peaks in good agreement with the expected size of the MS-s dimer (88 kDa) and tetramer (176 kDa). No monomeric MS-s was present, indicating that the protein associates to form homodimers and dimers of dimers.

Catalytic activity of MS-s

The ammonia-dependent CPSase activity of the recombinant *M. smithii* CPSase, MS-s, was measured in the coupled reaction with ATCase, as indicated in the *Experimental Procedures*. The enzyme catalyzes carbamoyl phosphate synthesis from ATP, ammonium chloride and bicarbonate, with a specific activity at 37°C of 77 ± 5.9 nmol/min/mg. Temperature had a very limited effect on the activity of MS-s, as the specific activity only decreased to 58.3 ± 4.2 nmol/min/mg when the assays were conducted at 22°C.

This small *M. smithii* CPSase also catalyzed the ATP-dependent partial reactions in accordance with the three step mechanism demonstrated for *E. coli* CPSase [Kothe *et al.*, 2005, Meister, 1989] (Table 1). The bicarbonate-dependent ATPase reaction in the presence (reactions 1 and 2) and absence (reaction 1 only) of ammonia measured at 22°C showed a ratio of 1.7:1, indicating that 2 ATP molecules are consumed in the carbamoyl phosphate synthesis when all of the substrates are present. Moreover, the CP-dependent ATP synthetase reverse reaction rate is very low (4.52 nmole/min/mg) relative to the ATP hydrolysis, representing 8% of the forward ATPase reaction in the presence of ammonia, as in the case of *A. aeolicus* CPSase [Ahuja *et al.*, 2001].

Enterococcus faecium carbamate kinase [Marina *et al.*, 1998] does not catalyze the first partial reaction, the bicarbonate dependent ATP hydrolysis in the absence of ammonia, whereas the second partial reaction measured in the reverse direction as a carbamoyl phosphate dependent ATP synthesis occurs at a very high rate (Table 1). In contrast, for MS-s, like *E. coli* CPSase [Rubio *et al.*, 1987] the rate of the bicarbonate dependent ATP hydrolysis is high relative to the carbamoyl phosphate-dependent ATP synthesis activity. The kinetic studies provided additional strong evidence that MS-s is a canonical CPSase, not a carbamate kinase.

Steady state kinetic parameters

Substrate saturation curves for ATP, NH_4Cl and $NaHCO_3$ of the recombinant MS-s were measured at 37°C (data not shown), and the kinetic parameters were calculated from the least squares fit to either the Michaelis-Menten or Hill equation. While both NH_4Cl and $NaHCO_3$ saturation curves follow Michaelis-Menten kinetics, the ATP saturation curve is slightly sigmoidal, with Hill coefficient of $n_H = 1.4 \pm 0.1$. The steady-state kinetic parameters (Table 2) indicated a relatively high apparent affinity for ATP (K_m=0.61 mM), 2- and 12-fold higher than the K_m(ATP) of *E. coli* SYN subunit (1.3 mM) [Rubio *et al.*, 1987] and *A. aeolicus* CPS.A-CPS.B complex (7.43 mM) [Ahuja *et al.*, 2001], respectively. The k_{cat} values for this substrate (0.043 s^{-1}) is 170-fold lower than the corresponding value (7.3 s^{-1}) for *E. coli* SYN subunit [Rubio *et al.*, 1987]. The apparent second-order rate constant k_{cat}/K_m for ATP (70.5 $M^{-1}s^{-1}$) is 21–23-fold higher than that for the other two substrates, NH_4Cl and $NaHCO_3$, indicating a high efficiency for ATP reaction. Moreover, this second order rate constant is 79-fold lower than that of *E. coli* SYN subunit (5600 $M^{-1}s^{-1}$). Surprisingly, the $K_m(NH_4Cl)$ value of MS-s (15.6 mM) is 13-fold lower than that for the *E. coli* enzyme (211 mM) [Huang and Raushel, 2000], indicating a high affinity for ammonia of this enzyme, while $K_m(NaHCO_3)$ is comparable to that of *E. coli* SYN subunit (10.8 mM). Furthermore, this small *M. smithii* CPSase shows similar k_{cat} and k_{cat}/K_m values for both $NaHCO_3$ and NH_4Cl substrates. While MS-s clearly catalyzed carbamoyl phosphate synthesis, the k_{cat} values were surprising low compared to other CPSases. Whether the kinetic parameters accurately reflect the intrinsic activity or are the result of instability of the protein or other factors involved in the assay are under investigation.

Mechanism of Carbamoyl Phosphate Synthesis

Besides the canonical CPSases, the only other enzymes that have been found to synthesize carbamoyl phosphate are the archaeal carbamate kinases from the hyperthermophilic organisms, *P. furiosus* and *P. abyssi*. These enzymes use ATP and carbamate formed chemically from ammonia and bicarbonate to synthesize carbamoyl phosphate. Several lines of evidence suggest that MS-s is much more closely related to the longer CPSases found in all mesophillic organisms, 1) MS-s is significantly larger (41 kDa) than either carbamate kinase or the hyperthermophilic enzymes (33 kDa), 2) MS-s exhibits no statistically significant sequence similarity to carbamate kinases, 3) the resides implicated in catalysis in *E. coli* CPSase are highly conserved in MS-s, whereas the enzyme lacks the carbamate kinase active site residues, 4) carbamate kinases do not catalyze the first partial reaction, the bicarbonate dependent ATPase activity, but rapidly catalyze the carbamoyl phosphate dependent ATP synthesis, while the reverse was observed for MS-s, 5) the stoichiometry of

the reaction catalyzed by carbamate kinases is one mole of ATP consumed in carbamoyl phosphate synthesis, whereas 2 ATPs are required for the carbamoyl phosphate synthesis catalyzed by MS-s, 6) the levels of ammonia are likely to be too low in the nitrogen limited environment of the gut to provide sufficient carbamate to sustain significant carbamoyl phosphate synthesis. Determination of the three dimensional structure of MS-s, now underway, should provide definitive evidence that the protein is more closely related to the mesophillic CPSases than carbamate kinase.

The question then arises as to how can a protein one third the size of the synthetase domain of *E. coli* CPSase catalyze the complex series of reactions (reactions 1–3) involved in carbamoyl phosphate synthesis. A model is proposed (Figure 6) that takes into consideration the overall structural and functional characteristics of MS-s, the smallest naturally occurring, active CPSase identified so far. As discussed above, MS-s can catalyze both partial reactions, the formation of carbamate from ATP, ammonia and bicarbonate and the ATP dependent synthesis of carbamoyl phosphate from carbamate. In principle, the carbamate synthesized once released from the complex could react with a second ATP to form carbamoyl phosphate (Figure 6A), but this process would be expected to be inefficient because carbamate is hydrolyzed in the aqueous milieu to ammonia and bicarbonate, setting up in effect a futile cycle resulting in wasteful ATP hydrolysis. We propose instead that the functional unit is the MS-s dimer (Figure 6B). In this species, the two MS-s monomers would be related to each other by a two fold axis of symmetry exactly analogous to the fused CPS.A and CPS.B domain in the *E. coli* enzyme. The model also postulates that, as in *E. coli* CPSase, the two active sites are connected by an intramolecular tunnel. When ATP, ammonia and bicarbonate bind to monomer (a) (Figure 6B) it becomes the site of synthesis of carbamate. Carbamate is then transferred to monomer (b) which now becomes the carbamoyl phosphate synthesis domain by defauIt. In a subsequent catalytic cycle the roles may be reversed such that subunit (b) catalyzes carbamate synthesis and subunit (a) converts carbamate to carbamoyl phosphate. In this scheme, carbamate remains sequestered within the complex and protected from hydrolysis.

While further structural and biochemical studies are required to validate this model, there is precedence for this mechanism in mammalian CPSase. It was shown that both CPS.A and CPS.B domains of mammalian CAD separately cloned and expressed in *E. coli* could each dimerize and catalyze both ATP-dependent reactions and the overall synthesis of carbamoyl phosphate [Guy *et al.*, 1997]. Moreover, the dissociation of CPS.A or CPS.B homodimers by high hydrostatic pressure abolished carbamoyl phosphate synthesis, while the dissociated subunits could still catalyze the CPSase partial reactions [Guy *et al.*, 1998].

Putative physiological function of MS-s

In adition to MS-s, *M. smithii* possesses an active, full length glutamine-dependent CPSase, MS-l, (unpublished data), so the question arises what selective advantage does the unusual CPSase, MS-s, provide for the organism. Ammonia is the major source of nitrogen in *M. smithii* for the biosynthesis of nucleotides, amino acids and many other metabolites. The organism has a specific ammonia transporter and two mechanisms for assimilation of ammonia, the glutamine synthetaseglutamate synthase and the glutamate dehydrogenase

pathways [Samuel *et al*, 2007]. However, the availability of ammonia is strictly limited in the intestine and there is a competition for this scare resource between *M. smithii* and *B. thetaiotaomicron*. This conclusion is supported by several lines of evidence. For example, analytical studies [Samuel *et al*, 2007] demonstrated that, in *M. smithii*, the ratio of glutamine to 2-oxoglutarate, a good indication of the nitrogen status of the organism, was reduced 32-fold when *M. smithii* was cocolonized with *B. thetaiotaomicron*. Moreover, when both organisms are present in the intestine, there is an appreciable up-regulation of the expression of enzymes involved in nitrogen assimilation in *M. smithii* [Samuel *et al*, 2007].

MS-s is a streamlined CPSase that is ideally suited to the task of capturing ammonia and converting it to pyrimidines and arginine. The kinetic studies showed that it has an appreciably higher affinity for ammonia than other CPSases. Moreover, the enzyme is also probably unregulated since the B3 or allosteric subdomain, the locus of regulation of all known CPSases, is not present in MS-s. While eukaryotic mitochondrial CPSase I, the enzyme that initiates the urea cycle, can be allosterically activated, there are no known allosteric inhibitors [Rubio and Cervera, 1995] presumably because it is essential in ureotylic animals to continuously and rapidly dispose of any ammonia formed via urea biosynthesis. Similarly, MS-s would be expected to be constitutively active if one of its major functions is to sequester ammonia, so that allosteric regulation would confer no advantage.

Conclusions

MS-s is a unique enzyme, the smallest functional CPSase discovered thus far and one that is only distantly related to other bacterial and archaeal CPSases. It consists of a catalytic domain, but lacks the module involved in allosteric regulation. The catalytically active species is an MS-s homodimer or larger species and the mechanism of carbamoyl phosphate synthesis appears to occur in three steps by the same mechanism utilized by the full length prokaryotic and eukaryotic CPSases. CPSase are postulated to be derived from an ancestral kinase resembling MS-s. Thus, the characterization of this enzyme may provide a glimpse of the evolution of CPSases, which are thought to have arisen by gene duplication, fusion and the recruitment of domains that confer regulatory functions. In addition to supplementing the function of the full length CPSase, MS-l, by bolstering the supply of pyrimidine nucleotides and arginine, MS-s may provide an additional mechanism for harvesting ammonia, a scare nutrient in the intestine. These minimal CPSases may be a characteristic of archaeal methanogens, since they are also present in *Methanothermobacter thermoautotrophicus* and *Methanosphaera stadtmanae*. Considering that there is apparently no mammalian counterpart of this unusual protein, MS-s may be an attractive drug target in the treatment of human obesity.

Experimental procedures

Materials — *Pfu* DNA polymerase, nucleotides, restriction enzymes, *Bam*HI and *Nco*I, thermosensitive alkaline phosphatase (FastAP), and T4 DNA ligase were from Fermentas Life Sciences; Ni^{2+}-ProBond resin was purchased from Invitrogen; aspartate, carbamoyl aspartate, antipyrine, diacetyl monoxime, triethoanolamine (TEA), phosphoenol pyruvate,

dimethyl suberimidate and the enzymes pyruvate kinase, lactate dehydrogenase, hexokinase, and glucose 6-phosphate dehydrogenase were from Sigma-Aldrich; *Aquifex aeolicus* aspartate transcarbamoylase (ATCase) recombinant enzyme was expressed in *E. coli* and purified as previously described [Purcarea *et al.*, 2003].

Strains and plasmids -—*Methanobrevibacter smithii ATCC35061* strain (DSM 861) was from DSMZ Bacteria Collection [Samuel *et al.*, 2007]. The *Escherichia coli* DH5α and BL21(DE3) strains and the pRSETC expression vector were from Invitrogen.

M. smithii* growth -—The methanogen M. smithii* ATCC35061 was cultivated anaerobically at 37°C in DSMZ 119 medium containing fatty acids and supplemented with DSMZ 320 salt solutions, in the presence of 80% H_2:20% CO_2 gas mixture [Samuel *et al.*, 2007]. Cultures of 20 ml were inoculated with 1 ml cultures under a N_2 atmosphere. The flasks were flushed every 24 hours with fresh H_2:CO_2 mixture, and the cell viability was analyzed by microscopy.

Cloning and expression -—*M. smithii* chromosomal DNA was isolated from a 20 ml culture, using the DNeasy Blood and Tissue Kit for genomic DNA extraction (Qiagen), with an additional cell lysis step using 50 units mutanolysin (Sigma). *The carB1* gene (YP_001272934) from *M. smithii* was amplified by PCR using 2.5 units *Pfu* DNA polymerase, 170 ng *M. smithii* chromosomal DNA as a template, and 100 pmol of 5MS-s (5'-GGAGATTGGATCCAAATTTTATTTATCGGTTCAAG-3') and 3MS-s (5'-GTGTTTAAGCCATGG TTAAATCAAATCTTCAACATATC-3') primers defining the 5' and 3' ends of *M. smithii carB1* gene, respectively. The DNA fragment was amplified after 30 cycles of 95°C for 45 sec, 52°C for 1 min and 72°C for 3 min each cycle, and purified with DNA Clean & Concentrator kit (Zymo Research). After digestion with *Bam*HI/*Nco*I, the gene (750 ng) was inserted into the pRSETC expression vector (130 ng) digested with the same restriction enzymes and dephosphorylated with thermosensitive alkaline phosphatase. Both strands of the resulting construct were sequenced using a Genetic Analyzer 3500 (Applied Biosystems). *M. smithii* CPS gene was expressed in *E. coli* BL21(DE3) after 5- hour induction at 20°C with 1 mM isopropyl-β-D-thiogalactopyranoside (IPTG).

Purification -—The recombinant *M. smithii* enzyme expressed in *E. coli* as an N-terminal fused protein with a 3-kDa His-tag polypeptide was purified in one step at 4°C by affinity chromatography. Cells from a 100-ml culture were resuspended in 3 ml of 50 mM TrisHCl, pH 8, containing 2 mM 2-mercaptoethanol and 1:100 protease inhibitor cocktail (Sigma), and disrupted by sonication six times for 30 seconds, using a Sonifier Cell disruptor W-350 (Bronson Sonic Power). The cell extract was centrifuged at 20,000 x *g* for 30 minutes, and the supernatant was applied to a 1-ml Ni^{2+}-ProBond column equilibrated with 50 mM TrisHCl, pH 8, and 200 mM NaCl (TN buffer). After 20 ml washes with the same buffer, the enzyme was eluted with 1-ml fractions of TN buffer containing increasing (50 mM, 100 mM, 200 mM and 500 mM) imidazole concentrations. The elution fractions were analyzed by electrophoresis on 12% SDS-PAGE gels. Fractions containing pure recombinant CPSase were collected and the buffer was exchanged to 50 mM TrisHCl, pH 8, 5 mM 2-

mercaptoethanol, using PD-10 Desalting columns (GE Healthcare), to eliminate imidazole and NaCl.

Chemical cross-linking -—Fractions containing 20 μg *M. smithii* CPSase in 100 mM triethanolamine, pH 8.5, 100 mM NaCl, were incubated with 10 mM dimethyl suberimidate [Davies *et al.*, 1970] for 0, 5, 10, and 15 minutes at room temperature in a total volume of 45 μl. The reaction was stopped by addition of 5 μl of 1 M TrisHCl, pH 8, and the crosslinked proteins were visualized by SDS-PAGE (10% gels)

Size exclusion chromatography -—Size exclusion chromatography was carried out at 4°C, using a Hiload 16/60 Superdex 200 prep grade column equilibrated with 50 mM TrisHCl, pH 8, containing 5 mM 2-mercaptoethanol. The column was loaded with 500- μl (5 mg) of the purified MS-s, and the protein was eluted at 1 ml/min with the equilibration buffer, monitoring the absorbance at 280 nm. The fractions containing the protein peaks were analyzed by SDS-PAGE.

Carbamoyl phosphate synthetase assay -—The ammonia-dependent CPSase activity was measured using the radioactive assay assay in which the CPSase reaction is coupled with *Aquifex aeolicus* aspartate transcarbamoylase (ATCase) [Ahuja *et al.*, 2001]. Expression and purification of the *A. aeolicus* ATCase were carried out as previously described [Purcarea *et al.*, 2003]. The reaction mixture contained 100 mM sodium [^{14}C] bicarbonate (100 dpm/μmol), 20 mM ATP, 22 mM $MgCl_2$ and 200 mM ammonium chloride, 50 mM TrisHCl, pH 8.0, 100 mM KCl, in the presence of 6 mM aspartate, pH 7, and 1 μg of purified *A. aeolicus* ATCase and various concentrations of recombinant MS-s CPSase, in a total volume of 0.3 ml. After a 20 minute incubation at 37°C, the reaction was stopped by addition of 0.7 ml 10% trichloracetic acid. After evaporation of the liquid phase at 95°C to decompose the unreacted bicarbonate, the radioactivity incorporated in the stable reaction product, carbamoyl aspartate, was measured after addition of 8 ml Aquasol scintillation liquid. Alternatively, the carbamoyl aspartate formed in the coupled reaction was measured by a colorimetric assay previously described [Purcarea *et al.*, 2001].

Partial Reactions -—*The bicarbonate-dependent ATPase reaction* was measured using a pyruvate kinase/lactate dehydrogenase coupled assay [Post *et al.*, 1990], by monitoring the rate of ADP synthesis in the presence and absence of ammonium chloride. The reaction was performed in a final volume of 0.5 ml containing 100 mM sodium bicarbonate, 20 mM ATP, 22 mM $MgCl_2$, 50 mM TrisHCl, pH 8.0, 100 mM KCl, 1 mM phosphoenolpyruvate, 0.2 mM NADH, 10 units of pyruvate kinase, and 20 units of lactate dehydrogenase, and, optionally, 200 mM ammonium chloride. The reaction rate was measured spectrophotometrically at 340 nm, and the concentration was calculated using NADH = 6.22 $M^{-1}.cm^{-1}$. *The carbamoyl phosphate-dependent ATP synthetase activity* was assayed by measuring the rate of ATP formation from ADP and carbamoyl phosphate in the coupled reaction with hexokinase/glucose-6-phosphate dehydrogenase, following a similar procedure [Miran *et al.*, 1991]. The reaction mixture contained 50 mM TrisHCl, pH 8.0, 100 mM KCl, 22 mM $MgCl_2$, 1 mM NAD, 20 mM ADP, 2 mM carbamoyl phosphate, 5 mM glucose, 20 units of hexokinase, and 10 units of glucose-6-phosphate dehydrogenase in a final volume of

0.5 ml. Both partial reactions were assayed at 22 °C and the initial rate was calculated from the time course up to 5 minutes time course.

Structure analysis and molecular modeling -—The genes encoding the CPSase subunits in *M. smithii* ATCC35061 genome sequence were identified by a BLAST-NCBI genome data base screening. Sequence analysis was performed using the genomic and proteomic software package ExPASy SIB Bioinformatics Resource Portal. Protein pair alignment was carried out with EMBOSS Needle-Alignment (EMBL-EBI) and multiple alignment was performed using ClustalW. Aminoacid sequence randomization was performed by using random protein sequence generator RandSeq software (ExPaSy). Modeling of the three-dimensional structure was carried out using Modeller 9v9 [Sali and Blundell, 1993], based on the 1BXR X-ray structure of *E. coli* CPSase in complex with the ATP analog AMPPNP [Thoden *et al.*, 1999]. Fifty models were generated and best candidate was chosen based on de DOPE (Discrete Optimized Protein Energy), zDOPE (normalized Discrete Optimized Protein Energy) and GA341 score. The energy minimization was performed with Gromos 96 implemented in Swiss PDB Viewer. The model was further refined by loop optimization using ModLoop [Fisher *et al.*, 2003] followed by energy minimization. In every round of optimization, at least 10 models where generated, followed by energy minimization. The quality of the model was assessed by the Ramachandran plot obtained with PROCHEK [Laskowski *et al.*, 1993], ERRAT2 [Colovos and Yeates, 1993], and ProSa [Sippl, 1993] programs. The superposition of MS-s model with 1BXR and the calculation of root mean square deviation (RMSD) where obtained using Swiss PDB Viewer [Guex and Peitsch, 1997]. The structures where visualized using the PyMol molecular Graphics System 0.99rc6 Schrodinger, LLC.

Acknowledgments

We thank Asmita Vaishnav for technical expertise and assistance. This work was supported by ANCSUEFISCDI Romania, PNII ID_1034 (Contract no. 1023/2009), NIH R01 grant GM/CA60371 and Wayne State University Provost's Research Stimulation Award.

Abbreviations

ATCase	aspartate transcarbamoylase
CarA	CPSase glutaminase subunit
CarB	CPSase synthetase subunit
CP	carbamoyl phosphate
CPSase	carbamoyl phosphate synthetase
TEA	triethanolamine
MS-s	*M. smithii* small CPSase
MS-l	*M. smithii* large CPSase
SYN	the 120 kDa CPSase synthetase subunit

References

1. Ahuja A, Purcarea C, Guy HI, Evans DR: A novel carbamoyl phosphate synthetase from Aquifex aeolicus. J Biol Chem 2001; 276: 45694–45703. [PubMed: 11574542]
2. Alonso E, Rubio V: Affinity cleavage of carbamoyl-phosphate synthetase I localizes regions of the enzyme interacting with the molecule of ATP that phosphorylates carbamate. Eur J Biochem1995; 229: 377–84. [PubMed: 7744060]
3. Anderson PM, Meister A: Evidence for an activated form of carbon dioxide in the reaction catalyzed by Escherichia coli carbamyl phosphate synthetase. Biochemistry 1965; 4: 2803–2809. [PubMed: 5326356]
4. Anderson PM: Carbamoyl-phosphate synthetase: an example of effects on enzyme properties of shifting an equilibrium between active monomer and active oligomer. Biochemistry 1986; 25: 5576–5582. [PubMed: 3535881]
5. Balch WE, Fox GE, Magrum LJ, Woese CL, Wolf RS: Methanogens: reevaluation of a unique biological group. Microbiol Rev 1979; 43: 260–296. [PubMed: 390357]
6. Belay N, Mukhopadhyay B, De Macario EC, Galask R, Daniels L: Methanogenic bacteria in human vaginal samples. J Clin Microbiol 1990; 28: 1666–1668. [PubMed: 2199527]
7. Belay N, Johnson R, Rajagopal BS, De Macario ES, Daniels L: Methanogenic bacteria from human dental plaque, Appl Environ Microbiol 1988; 54:600–603. [PubMed: 3355146]
8. Buck S, Hansen EE: Genomic and metabolic adaptations of Methanobrevibacter smithii to the human gut. Proc Natl Acad Sci U.S.A 2007;104:10643–10648. [PubMed: 17563350]
9. Bult CJ, White O, Olsen GJ, Zhou L, Fleischmann RD, Sutton GG, Blake JA, FitzGerald LM, Clayton RA, Gocayne JD, Kerlavage AR, Dougherty BA, Tomb FJ, Adams MD, Reich CI, Overbeek R, Kirkness EF, Weinstock KG, Merrick JM, Glodek A, Scott JL, Geoghangen NS, Venter JC: Complete genome sequence of the methanogenic archaeon, Methanococcus jannaschii. Science 1996; 273: 1058–1073. [PubMed: 8688087]
10. Colovos C, Yeates TO: Verification of protein structures: patterns of nonbonded atomic interactions. Protein Sci 1993; 2: 1511–1519. [PubMed: 8401235]
11. Davies GE, Stark GR: Dimethyl suberimidate, a cross-linking reagent, in studying the subunit structure of oligomeric proteins. Proc Natl Acad Sci USA 1970; 66: 651–656. [PubMed: 4913206]
12. Dridi B, Raoult D, Drancourt M: Archaea as emerging organisms in complex human microbiomes. Anaerobe 2011; 17: 56–63. [PubMed: 21420503]
13. Durbecq V, Legrain C, Roovers M, Piérard A, Glansdorff N: The carbamate kinase-like carbamoyl phosphate synthetase of the hyperthermophilic archaeon Pyrococcus furiosus, a missing link in the evolution of carbamoyl phosphate biosynthesis. Proc Natl Acad Sci U S A 1997; 94:12803–12808. [PubMed: 9371756]
14. Fiser A, Sali A: ModLoop: automated modeling of loops in protein structures. Bioinformatics 2003; 19: 2500–2501 [PubMed: 14668246]
15. Fresquet V, Mora P, Rochera L, Ramón-Maiques S, Rubio V, Cervera J. Site-directed mutagenesis of the regulatory domain of Escherichia coli carbamoyl phosphate synthetase identifies crucial residues for allosteric regulation and for transduction of the regulatory signals. J Mol Biol 2000: 299: 979–991. [PubMed: 10843852]
16. Guillou F, Rubino SD, Markovitz RS, Kinney DM, Lusty CJ: Escherichia coli carbamoyl-phosphate synthetase: domains of glutaminase and synthetase subunit interaction. Proc Natl Acad Sci U S A 1989; 86:8304–8308. [PubMed: 2682645]
17. Guex N, Peitsch MC: SWISS-MODEL and the Swiss-PdbViewer: An environment for comparative protein modeling. Electrophoresis 1997; 18: 2714–2723. [PubMed: 9504803]
18. Guy HI, Evans DR: Function of the major synthetase subdomains of carbamyl-phosphate synthetase. J Biol Chem 1996; 271:13762–13769. [PubMed: 8662713]
19. Guy HI, Bouvier A, Evans DR: The Smallest Carbamoyl-phosphate Synthetase. J Biol Chem 1997; 272: 29255–29262 [PubMed: 9361005]
20. Guy HI, Schmitt B, Hervé G, Evans DR: Pressure-induced dissociation of carbamoyl-phosphate synthetase domains. The catalytically active form is dimeric. J Biol Chem 1998; 273:14172–14178. [PubMed: 9603918]

21. Horz HP, Conrads G: The discussion goes on: What is the role of Euryarchaeota in humans, Archaea DOI: 10.1155/2010/967271
22. Huang X, Raushel FM: An engineered blockage within the ammonia tunnel of carbamoyl phosphate synthetase prevents the use of glutamine as a substrate but not ammonia. Biochemistry 2000; 39: 3240–3247. [PubMed: 10727215]
23. Kim J, Raushel FM: Allosteric Control of the Oligomerization of Carbamoyl Phosphate Synthetase from Escherichia coli. Biochemistry, 2001; 40: 11030–11036 [PubMed: 11551199]
24. Kothe M, Purcarea C, Guy HI, Evans DR, Powers-Lee SG: A Novel Carbamoyl-Phosphate Synthetase from Aquifex aeolicus. J Biol Chem 2005; 14: 37–44.
25. Laskowski RA, MacArthur MW, Moss DS, Thornton JM: PROCHECK: a program to check the stereochemical quality of protein structures. Journal of Applied Crystallography, 1993; 26: 283–291
26. Legrain C, Demarez M, Glansdorff N, Pierard A: Ammonia – dependent synthesis and metabolic channelling of carbamoyl phosphate in the hyperthermophilic archaeon Pyrococcus furiosus. Microbiol 1995; 141: 1093–1099.
27. Marina A, Uriarte M, Barcelona B, Fresquet V, Cervera J, Rubio V: Carbamate kinase from Enterococcus faecalis and Enterococcus faecium: cloning of the genes, studies on the enzyme expressed in Escherichia coli, and sequence similarity with N-acetyl-L-glutamate kinase. Eur J Biochem 1998; 253: 280–291. [PubMed: 9578487]
28. Meister A: Mechanism and regulation of the glutamine–dependent carbayl phosphate synthetase of Escherichia coli. Adv Enzymol Relat Areas Mol Biol 1989; 62: 315–374. [PubMed: 2658488]
29. Miller TL, Wolin MJ, De Macario EC, Macario AJ: Isolation of Methanobrevibacter smithii from human feces. Appl Environ Microbiol 1982; 43: 227–232. [PubMed: 6798932]
30. Million M, Maraninchi M, Henry M., Armougom F, Richet H, Carrieri P, Valero R, Raccah D, Vialettes B, Raoult D: Obesity – associated gut microbiota is enriched in Lactobacillus reuteri and depleted in Bifidobacterium animalis and Methanobrevibacter smithii. Int J Obes DOI: 10.1038/ijo.2011.153
31. Miran SG, Chang SH, Raushel FM: Role of the four conserved histidine residues in the amidotransferase domain of carbamoyl phosphate synthetase. Biochemistry 1991; 30: 7901–7909. [PubMed: 1868065]
32. Nava GM, Caronero F, Croix JA, Greenberg E, Gaskins HR: Abundance and diversity of mucosa-associated hydrogenotrophic microbes in the healthy human colon. ISME J DOI: 10.1038/ismej.2011.90.
33. Nyunoya H, Lusty CJ: The carB gene of Escherichia coli: a duplicated gene coding for the large subunit of carbamoyl-phosphate synthetase. Proc Natl Acad Sci USA 1983; 80: 4629 – 4633. [PubMed: 6308632]
34. Paulus TJ, Switzer RL: Caracterization of pyrimidine-repressible and arginine-repressible carbamyl phosphate synthetase from Bacillus subtilis. J Bacteriol 1979; 137: 82–91. [PubMed: 216664]
35. Plottel CS, Blaser MJ: Microbiome and malignancy. Cell Host Microb 2011; 10: 324–335.
36. Popa E, Rusu A, Zamfir M, Dumitru L, Purcarea C: An ammonia-metabolizing enzyme from the human archaeon Methanobrevibacter smithii might represent a missing link in the evolution of carbamoyl phosphate synthetases. Biotechol & Biotechol Eq 2009; 23:533–537.
37. Post LE, Post DJ, Raushel FM: Dissection of the functional domains of Escherichia coli carbamoyl phosphate synthetase by site-directed mutagenesis. J Biol Chem 1990; 265:7742–7747. [PubMed: 2186028]
38. Purcarea C, Simon V, Prieur D, Hervé G: Purification and characterization of carbamylphosphate synthetase from the deep–sea hyperthermophilic archaebacterium Pyrococcus abyssi. Eur J Biochem 1996; 236: 189–199. [PubMed: 8617264]
39. Purcarea C, Hervé G, Cunin R, Evans DR: Cloning, expression and structure analysis of carbamat kinase-like carbamoyl phosphate synthetase from Pyrococcus abyssi. Extremophiles 2001; 5: 229–239. [PubMed: 11523892]

40. Purcarea C, Ahuja A, Lu T, Kovari L, Guy HI, Evans DR: Aquifex aeolicus aspartate transcarbamoylase, an enzyme specialized for the efficient utilization of unstable carbamoyl phosphate at elevated temperature. J Biol Chem 2003; 278: 52924–52934. [PubMed: 14534296]
41. Rubio SD, Nyunoya H, Lusty CJ: In vivo synthesis of carbamyl phosphate from NH_3 by the large subunit of Escherichia coli carbamyl phosphate synthetase. J Biol Chem 1987; 262: 4382–4386. [PubMed: 3549732]
42. Rubio V, Cervera J, Lusty CJ, Bendala E, Britton HG. Domain structure of the large subunit of Escherichia coli carbamoyl phosphate synthetase. Location of the binding site for the allosteric inhibitor UMP in the COOH-terminal domain. Biochemistry 1991 30:1068–1075. [PubMed: 1989678]
43. Rubio V, Cervera J: The carbamoyl-phosphat synthetase family and carbamate kinase: structure – function studies. Biochem Soc Trans 1995; 23: 879–83. [PubMed: 8654858]
44. Šali A, Blundell TL: Comparative protein modelling by satisfaction of spatial restraints. J Mol Biol 1993; 234: 779–815. [PubMed: 8254673]
45. Samuel BS, Gordon JI: A humanized gnotobiotic mouse model of host-archaeal-bacterial mutualism. Proc Natl Acad Sci USA 2006; 103: 10011–10016. [PubMed: 16782812]
46. Samuel BS, Hansen EE, Manchester JK, Coutinho PM, Henrissat B, Fulton R, Latreille P, Kim K, Wilson RK, Gordon JI: Genomic and metabolic adaptations of Methanobrevibacter smithii to the human gut. Proc Natl Acad Sci U.S.A 2007; 104: 10643–10648. [PubMed: 17563350]
47. Sippl MJ: Recognition of Errors in Three-Dimensional Structures of Proteins. 1993; Proteins; 17: 355–362 [PubMed: 8108378]
48. Stams AJ: Metabolic interactions between anaerobic bacteria in methanogenic environments. Antonie van Leeuwenhoek 1994; 66: 271–294. [PubMed: 7747937]
49. Thoden JB, Holden HM, Wesenberg G, Raushel FM, Rayment I: The structure of carbamoyl phosphate synthetase: a journey of 96 Å from substrate to product. Biochemistry 1997; 36: 6305–6316. [PubMed: 9174345]
50. Thoden JB, Wesenberg G, Raushel FM, Holden HM: Carbamoyl phosphate synthetase: closure of the B-domain as a result of nucleotide binding. Biochemistry 1999; 38: 2347–2357. [PubMed: 10029528]
51. Trotta PP, Burt ME, Haschemeyer RH, Meister A: Reversible dissociation of carbamyl phosphate synthetase into a regulated synthesis subunit and a subunit required for glutamine utilization. Proc Natl Acad Sci. USA 1971; 68: 2599–2603. [PubMed: 4944634]
52. Uriarte M, Marina A, Ramon-Maiques S, Rubio V, Durbecq V, Legrain C, N. Glansdorff N: Carbamoyl phosphate synthesis: carbamate kinase from Pyrococcus furiosus. Methods Enzymol 2001; 331: 236–247. [PubMed: 11265466]
53. Yang H, Park SM, Nolan WG, Lu CD, Abdelal AT: Cloning and characterization of the arginine – specific carbamoyl-phosphate synthetase from Bacillus stearothermophilus. Eur J Biochem 1997; 249: 443–449. [PubMed: 9370352]

(A)

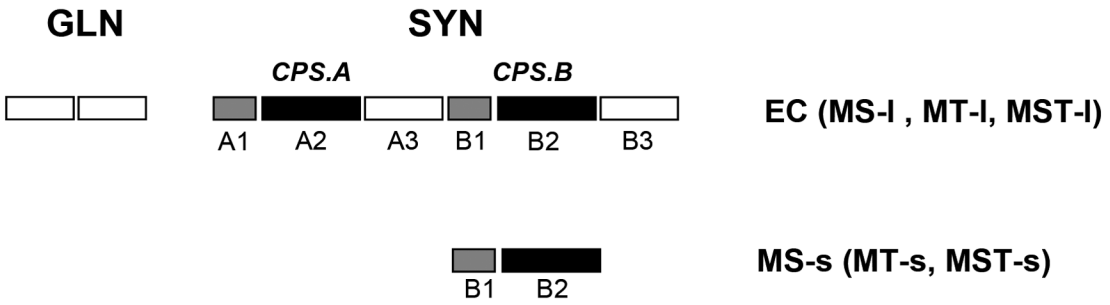

(B)

MST-s	MT-s	MS-l	MST-l	MT-l	EC	PA	% identity
48.1	47.6	23.5	24.2	19.1	20.1	11.5	**MS-s**
	46.9	24.3	25.7	14.5	25.3	13.3	**MST-s**
		27.0	25.9	21.2	21.8	14.5	**MT-s**
			73.5	73.1	52.0	5.5	**MS-l**
				70.7	50.3	6.2	**MST-l**
					52.8	8.3	**MT-l**
						5.8	**EC**

Figure 1. MS-s sequence identity and domain structure

(**Panel A**) Domain and subdomain organization of MS-s and the full length SYN subunits. The full length SYN domain consists of homologous CPS.A and CPS.B domains each of which are comprised of subdomains designated A1, A2, A3 and B1, B2, B3 subdomains, respectively, of the *E. coli* SYN subunit. (**Panel B**) Protein sequence identity (%) was calculated by pair-wise alignment of CPSase synthetase subunits, as indicated in the *Experimental Procedures*. The proteins analyzed in both panels are: *M. smithii* small (MS-s) and large (MS-l) SYN; *Methanothermobacter thermoautotrophicus* small (MT-s) and large

(MT-l) SYN, *Methanosphaera stadtmanae* small (MST-s) and large (MST-l) SYN; *E. coli* (EC) SYN; *Pyroccocus abyssi* (PA) CK-like CPSase.

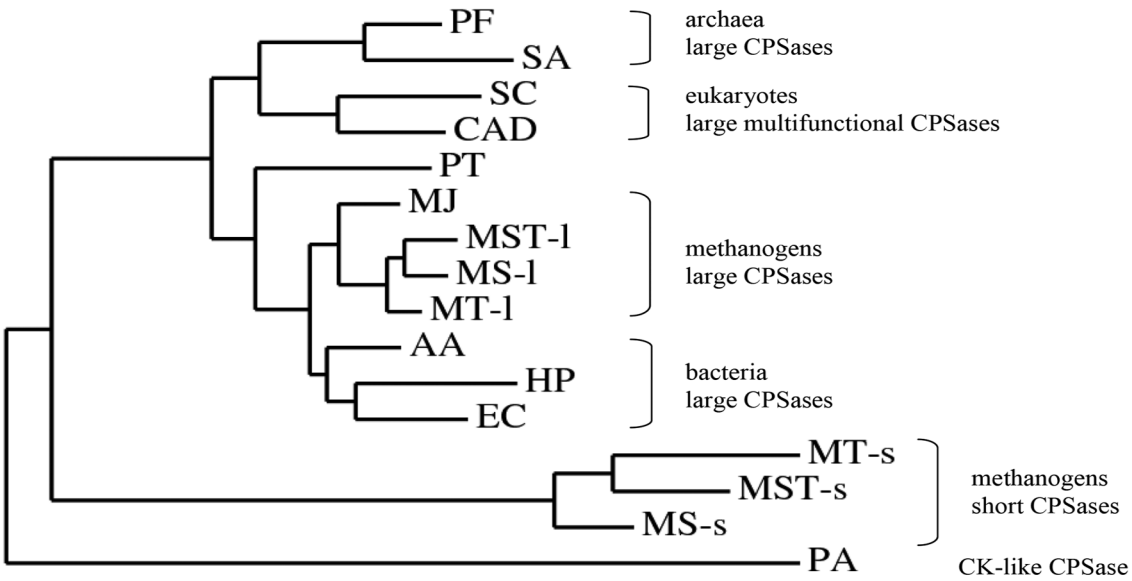

Figure 2. Phylogenetic tree of CPS SYN subunits

The phylogenetic tree was constructed as indicated in the *Experimental Procedures*, using the amino acid sequences of CPS SYN subunits or domains from the methanogens, *M. smithii* small (MS-s) and large (MS-l); *Methanothermobacter thermoautotrophicus* small (MT-s) and large (MT-l); *Methanosphaera stadtmanae* small (MST-s) and large (MST-l); *Methanothermococcus jannaschii* (MJ); *Aquifex aeolicus* (AA); *E. coli* (EC); *Helicobacter pylori* (HP); the archaea, *Picrophilus torridus* (PT); *Sulfolobus acidocaldarius* (SA); *Pyrococcus furiosus* (PF); *Pyroccocus abyssi* (PA) CK-like CPSase; *Saccharomyces cerevisiae* (SC) pyrimidine-specific enzyme and the hamster pyrimidine biosynthetic multifunctional protein (CAD).

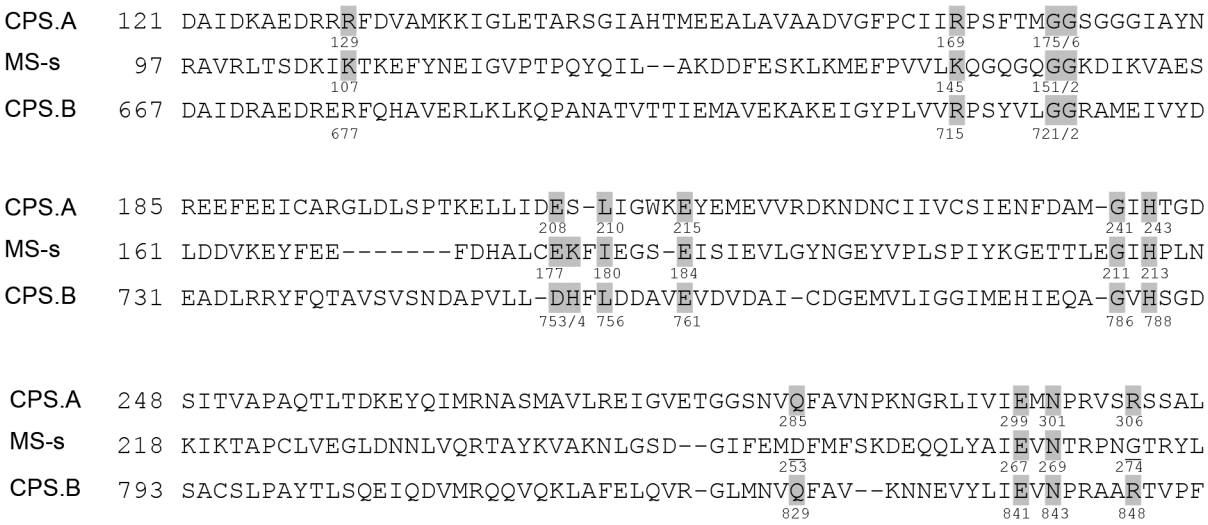

E. coli		*M. smithii*	Functional Interactions
CPS.A	**CPS.B**	**MS-s**	
Arg129	(Arg677)	Lys107	α and β phosphates AMP-PNP
Arg169	Arg715	Lys145	α phosphate of AMP-PNP
Gly175	Gly721	Gly151	γ phosphate of AMP-PNP
Gly176	Gly722	Gly152	β phosphate of AMP-PNP
Glu208	Asp753	Glu177	amino group of adenine ring
(Ser209)	His754	Lys178	amino group of adenine ring
Leu210	Leu756	Ile180	purine ring
Glu215	Glu761	Glu184	2’ and 3’ hydroxyl of ribose
Gly241	Gly786	Gly211	2’ hydroxyl of ribose
Gln285	Gln829	Asp253*	α phosphate of AMP-PNP / Mg^{2+}
Glu299	Glu841	Glu267	binds Mg^{2+}
Asn301	Asn843	Asn269	binds Mg^{2+}
Arg306	Arg848	Gly274*	γ phosphate of AMP-PNP

Figure 3. Active site conservation of MS-s

The alignment of MS-s with *E. coli* CPS.A and CPS.B domains was carried out as indicated in the *Experimental Procedures*. The residues that interact with the bound substrates AMPPNP and Mg^{+2} and those that are part of the loop closing the active site identified in the X-ray structure of *E. coli* CPSase [Thoden *et al.*, 1999] are indicated in both the alignment and table. The interacting residues in each *E. coli* subdomain are shaded grey and their position (residue number) is indicated. Residues in MS-s that are not conserved are underlined in the alignment and indicated by (*) in the table. The corresponding active site residues that are not interacting in CPS.A or CPS.B are enclosed in parenthesis.

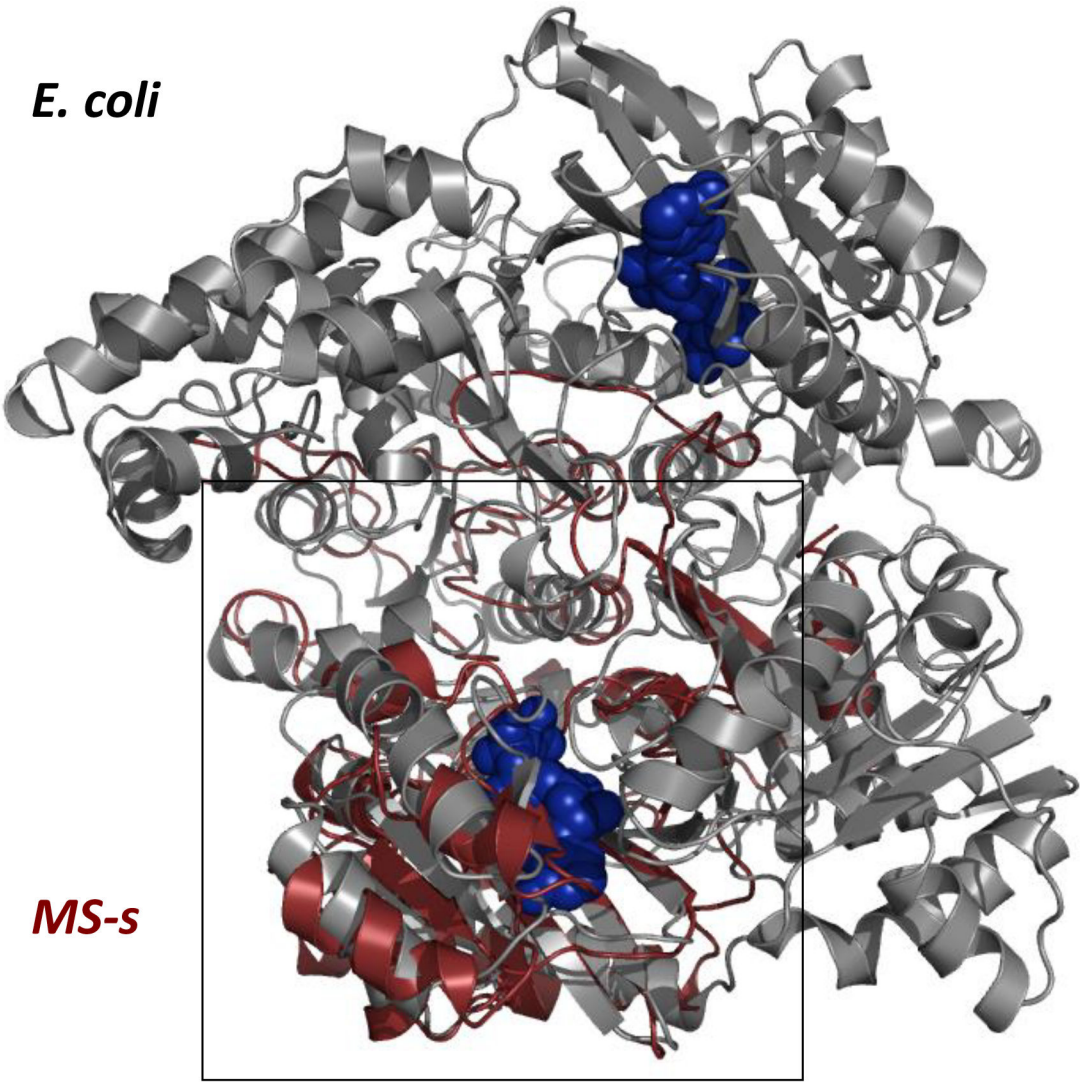

Figure 4. Molecular modeling of MS-s

Superposition of the modeled three dimensional structure of MS-s (red) with the *E. coli* CPSase 1BXR [Thoden *et al.*, 2009] X-ray structure (grey). The position of the ATP analog AMPPNP [Thoden *et al.*, 2009] is shown (blue) bound to both CPS.A and CPS.B domains of the *E. coli* enzyme; the box indicates the region of the carbamate phosphorylation domain in *E. coli* CPSase, corresponding to B1–B2 subdomains.

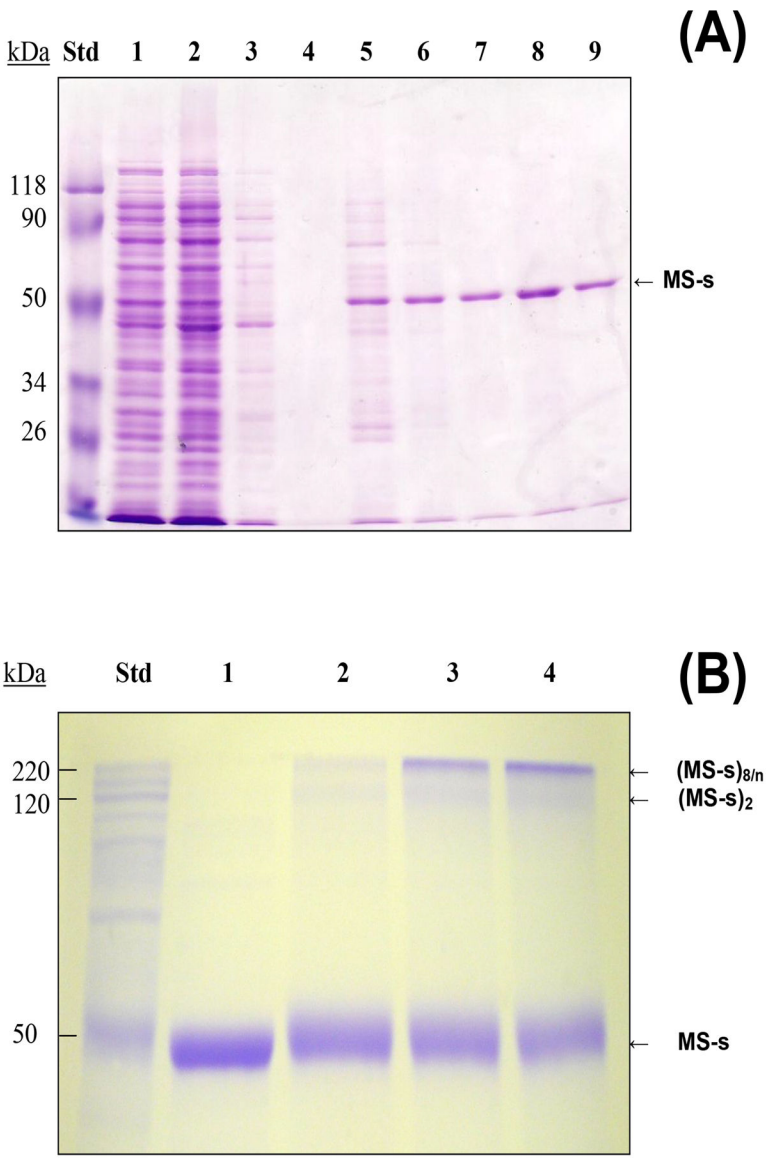

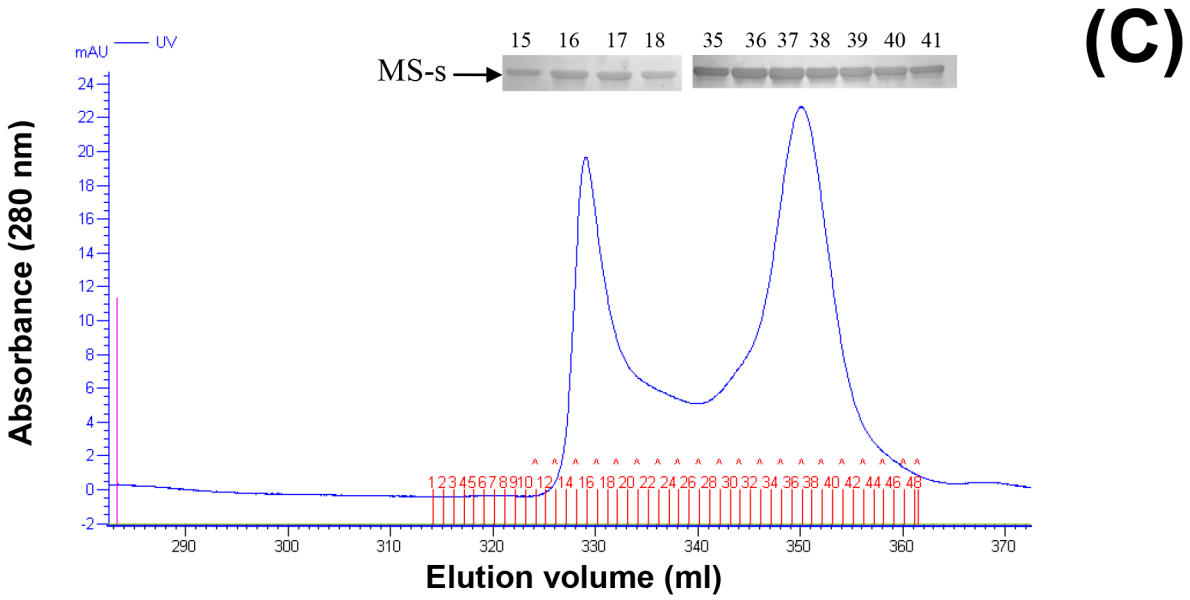

Figure 5. MS-s purification and oligomeric structure determination

(**Panel A**) Purification of the recombinant MS-s was carried out by affinity chromatography on Ni^{2+}-Probond resin as described in the *Experimental Procedures*, and the elution fractions were analyzed by 12% SDS-PAGE. The lanes correspond to the molecular weight marker (Std), fractions 1–3 eluted with TN buffer (50 mM TrisHCl, pH 8, 200 mM NaCl), fractions 4–6 eluted with TN buffer containing 50 mM imidazole and fractions 7–9 eluted with TN buffer containing 100 mM imidazole. (**Panel B**) Chemical cross-linking was carried out at 22°C for 0 min, 5 min, 10 min and 15 min (lanes 1–4) using 20 μg recombinant MS-s in 100 mM TEA buffer pH 8.5, 100 mM NaCl, and 10 mM dimethylsuberimidate. The reaction mixture was quenched with 100 mM TrisHCl, pH 8, and analyzed by 10% SDS-PAGE. (**Panel C**) Size exclusion chromatography was carried out as indicated in the *Experimental Procedures*. The elution profile was obtained by measuring the absorbance at 280 nm. The peak fractions (fractions 15–18 and 35–41) were analyzed by 10% SDS-PAGE and found to contain MS-s.

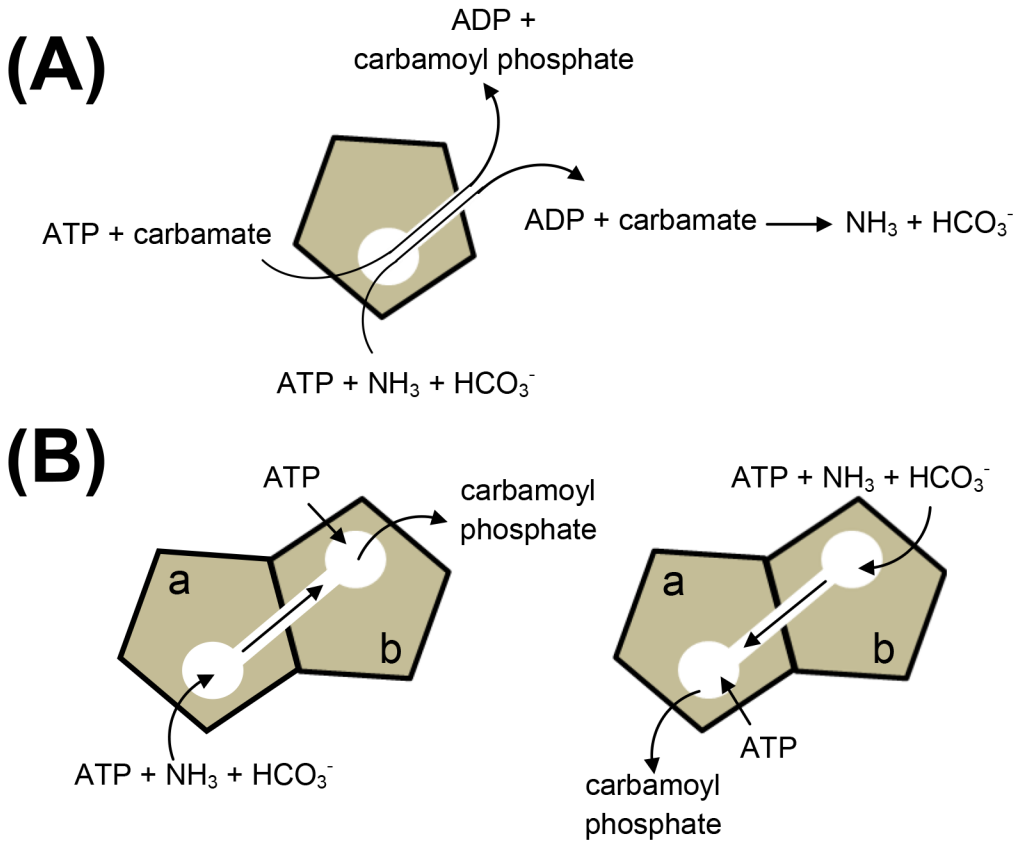

Figure 6. Functional model of MS-s

A schematic representation of carbamoyl phosphate (CP) synthesis by MS-s. (**Panel A**) Carbamate is synthesized from bicarbonate, ammonia and ATP, released from the enzyme, and then binds once again where it is phosphorylated by a second ATP molecule forming carbamoyl phosphate. This process would be expected to be inefficient since carbamate once released from the complex would be degraded to bicarbonate and ammonia. **Panel B**) The synthesis of carbamate is catalyzed by one of the monomers in the MS-s dimer (a) which binds bicarbonate, ammonia and ATP, the carbamate is sequestered and transferred to the second monomer (b) which catalyzes the phosphorylation of carbamate to form carbamoyl phosphate. In a subsequent catalytic cycle, the roles of subunits a and b may be reversed.

Table 1.

ATP-dependent partial reactions

Enzyme	HCO_3^--dependent ATPase, nmol/min/mg		CP-dependent ATP synthetase nmol/min/mg
	$+NH_3$	$-NH_3$	
M. smithii MS-s	5884	3582	481
E. faecium CKase *	427	8	4,533
E. coli CPSase **	2,0008400	400850	390850

ADP and ATP formation catalyzed by *M. smithii* small CPSase (MS-s) was measured at 22 °C as indicated in the *Experimental Procedures*. The specific activity and standard deviations were calculated from three experiments.

* Results from [Marina *et a*l, 1998];

** Results from [Miran *et al.*, 1991].

Table 2.

Steady state kinetic parameters

Substrate	K_m mM	V_{max}, nmol/ min/mg	k_{cat} s^{-1}	k_{cat}/K_m $M^{-1}?s^{-1}$
*ATP**	0.6180.01	6281	0.04380.003	70.5
NH_4Cl	15.682.6	7583	0.05280.003	3.3
Bicarbonate	14.583.6	6487	0.04480.006	3.0

The steady state kinetic parameters were determined at 37°C, from the ATP, ammonium chloride and sodium bicarbonate saturation curves of MS-s (10 μg) in the coupled reaction with *A. aeolicus* ATCase as indicated in the *Experimental Procedures*.

*The sigmoidal ATP saturation curve was fit to the Hill equation, so the K_m was replaced with $[S]_{0.5}$. The steady state kinetic parameters and standard deviations were obtained by a least squares fit of eight data points in each saturation curve.